The Rheological Characterisation of Emulsions as Saliva Substitutes

Sara M. Hanning[1], Tao Yu[2], Jules A. Kieser[1], David S. Jones[2], Gavin P. Andrews[2] and Natalie J. Medlicott[1]

[1] University of Otago, Dunedin, New Zealand.
[1] Queen's University Belfast, Belfast, Northern Ireland.

ABSTRACT

This study investigated emulsions for use as saliva substitutes in patients with xerostomia. Rheological properties of these emulsions changed as a function of frequency and small-angle light scattering (SALS) was investigated as a tool to quantify changes to droplet microstructure at different frequencies. SALS was successfully used to differentiate between formulations, but was unable to detect changes in droplet microstructure within compositions. Viscous behaviour of emulsions at lower frequencies may improve lubrication of the oral cavity whereas elasticity at higher frequencies may improve retention during chewing and swallowing.

INTRODUCTION

The oral cavity is a complex, dynamic environment[1,2] with different forces and stresses occurring simultaneously on different surfaces and in different functional entities within the mouth[3,4]. Saliva is a complex, viscoelastic fluid that is continually secreted at a flow rate and composition dependent on a myriad of external factors. Salivary hypofunction is the objective reduction in flow rate or altered composition of stimulated or unstimulated saliva[5,6] and is often associated with xerostomia, defined as the subjective feeling of dry mouth. Current treatment options for xerostomia are limited, aiming to relieve oral discomfort by keeping the mouth moist[7,8].

Previous research has shown that emulsions consisting of rice bran oil (RBO), soy lecithin and water may offer improved relief in patients with xerostomia. These compositions exhibited rheological properties that were frequency-dependent, where viscous behaviour dominating at frequencies below 5 Hz and elastic behaviour dominating at higher frequencies[9]. This feature was thought to be beneficial in a saliva substitute, with viscous behaviour improving lubrication at rest and elastic behaviour improving retention during high-shear tasks such as speaking and swallowing. Reversible peaks in G' and G" were observed in many formulations, with the critical frequency at which the peak occurred depending upon the relative concentration of each component. This was thought to be related a frequency-dependent temporary aggregation of the dispersed phase.

The purpose of this study was to explore changes in the microstructure of these RBO and lecithin systems as a function of frequency. Small-angle light scattering (SALS) was investigated as a tool to quantify changes to droplet microstructure at different frequencies.

MATERIALS AND METHODS

Preparation of compositions

A surfactant mix (SM) was prepared by mixing soybean lecithin (Lipoid GmBH, Ludwigshafen, Germany) and propylene glycol (Sigma, St Louis, MO, USA) at a weight ratio of 1:1 w/w until a transparent mixture was achieved.

Compositions were prepared as previously described[9] by magnetically stirring different ratios of rice bran oil (RBO, Bespoke Foods, London, UK), SM and distilled water. The ratio of each component varied by 10% w/w such that 66 different combinations were possible. Selected compositions containing up to 60% w/w SM, 30% w/w RBO and distilled water were examined using laser diffraction and SALS.

Droplet size analysis of compositions

The droplet size distribution of compositions was investigated using a laser diffraction particle sizer (LA-950V2, Horiba Instruments Inc., Irvine, CA, USA) with distilled water as the dispersion media. To ensure even distribution of each composition, 0.1 mL mixture was added to 0.9 mL water and gently mixed with a 360° rotary mixer. This was added drop-wise to the dispersion media in the particle sizer to achieve the desired red transmission between 92% and 89% (approximately 300 µL). Volume mean diameter was calculated from three measurements and the coefficient of variation (CV) was determined by dividing the standard deviation by the mean volume distribution of 10% (D_{10}), 50% (D_{50}; also the median) and 90% (D_{90}) of the droplets.

Compositions were examined under both polarised and non-polarised light using a Motic BA 300Pol light microscope (Motic Incorporation, Hong Kong) coupled with a Moticam 2300 digital camera (Motic Incorporation, Hong Kong). Droplet size was then estimated using ImageJ 10.2 software (Public Domain Java Image Processing Programme, National Institute of Health, USA).

Scattering pattern of compositions

Oscillatory rheological analyses were performed at 20°C to reduce evaporation of the compositions during the testing period, using a DHR Series rotational rheometer (T.A. Instruments, Surrey, England). A SALS accessory (T.A. Instruments, Surrey, England) was attached to the top of the rheometer with a Class II 0.95 mW diode laser (with wavelength of 0.6328 µm, 1.1 mm circular beam and beam divergence of 0.7 mrad). A 50 mm quartz parallel plate geometry was used with a fixed gap of 1000 µm and stress amplitude of 5 Pa.

Calibration of the SALS set-up was performed according to the T.A. Instruments operating manual (Surrey, England), using a polystyrene bead suspension (Fluka Analytical, Buchs, Switzerland) with calibrated particle diameter of 3.113 µm, CV of 1.97% and refractive index of 1.5905, diluted to obtain a microparticle concentration of 0.05% w/v. To determine correction factors for the observed data, the predicted scattering pattern (relative intensity as a function of scattering angle, θ) was calculated using MiePlot 4.3 (Philip Laven, Geneva, Switzerland) and overlaid on the plot of observed scattering pattern. A correction factor (F_c) was calculated to adjust for pixel position relative to the light source (Eq. 1). Intensity (I) was corrected (I_{corr}) using F_c and a y-shift correction factor (F_y), which was manually adjusted until the first peak of the observed scattering pattern had the same magnitude as the first peak of the predicted scattering pattern (Eq. 2). The measured radius in pixels (r) was converted to scattering angle (θ) using Eq. 3, where the optics factor (F_o) was adjusted until the first peak of the observed scattering pattern overlapped the first peak of the predicted pattern. These correction factors were then applied to the sample data.

$$F_C = \left(\cos\frac{0\pi}{180}\right)^3 \quad (1)$$

$$I_{corr} = \frac{(I * F_y)}{F_C} \quad (2)$$

$$0 = \frac{180.\arctan(r.F_g)}{\pi} \quad (3)$$

To obtain an optimal dilution factor, a 5 µm microparticle size standard suspension (Fluka Analytical, Buchs, Switzerland) was diluted to obtain particle concentrations of 0.1%, 0.05% and 0.03% (w/v). A step sweep was conducted on each composition within a frequency range of 0.1 to 1.0 Hz. Approximately 1.96 mL mixture was applied to the lower stationary plate of the rheometer and allowed to equilibrate for three minutes. Each composition was held for 30 seconds at pre-determined frequencies of 0.1, 2, 4, 6, 8 and 10 Hz so that five images could be captured using a LuCam Capture camera (Lumenera Corporation, Nepean, ON, Canada). These were averaged using ImageJ 10.2 (Public Domain Java Image Processing Programme, National Institute of Health, USA) and the averaged water background image was subtracted. Radial profile angle was determined and a correction factor was applied to normalise the intensity as a function of scattering angle. This procedure was then repeated using Intralipid® (Pharmatel Fresenius Kabi AB, Sweden) as a standard emulsion, diluted by a factor of 200, 500, 1000, 2000 and 4000 using distilled water. Intralipid® contains 20% w/v oil, so these dilution factors corresponded with an oil concentration (w/v) of 0.1%, 0.04%, 0.02%, 0.01% and 0.05%, respectively. From these preliminary tests, a target emulsion concentration between 0.02% and 0.04% (w/v) was identified for the SALS analysis.

The selected test compositions contained up to 30% w/w RBO and between 30% and 60% w/w water. To obtain an emulsion concentration within the desired range of 0.02% to 0.04% w/v, each composition was diluted by a factor of 2000 using distilled water and mixed gently using a 360° rotary mixer. Approximately 1.96 mL sample was then applied to the lower stationary plate of the rheometer and allowed to equilibrate for three minutes before a step sweep was conducted within a frequency range of 0.1 to 10 Hz. Each composition was held for 30 seconds at pre-determined frequencies of 0.1, 2, 4, 6, 8 and 10 Hz so that images could be captured. Five images were obtained at each frequency using a LuCam Capture camera (Lumenera Corporation, Nepean, ON, Canada). These were averaged using ImageJ 10.2 (Public Domain Java Image Processing Programme, National Institute of Health, USA) and the averaged water background image was subtracted. Radial profile angle was determined and data was adjusted using the correction factors described above to gain adjusted intensity as a function of scattering angle.

Statistical analysis

The droplet size diameters of compositions were compared using a one-way analysis of variance (ANOVA) with Bonferroni post hoc corrections. Data were analysed using R (version 3.0.3, www.r-project.org) coupled with RStudio (version 0.98.501, www.rstudio.com).

RESULTS AND DISCUSSION

Droplet size analysis of compositions

The CV values of D_{10}, D_{50} and D_{90} for each composition were all less than 5%, except for that consisting of 10% RBO, 60% SM and 30% water (w/w), which had a CV of 22% at D_{10} (Table 1). These were below the precision limits indicated by the United States Pharmacopoeia of 10% for D_{50} and 15% for D_{10} and D_{90}, doubled if samples are

under 10 µm[10]. Emulsions had bimodal or trimodal distribution, with droplet size dependent upon composition. Droplet size distribution correlated with images obtained using light microscopy, although droplet diameters less than 2 µm were not detectable with the light microscopy method (Fig. 1).

Table 1. Mean droplet diameter D_{10}, D_{50} and D_{90} (± SD) and CV of different concentrations (conc.) of RBO (O), SM and water (W) (n = 3; * denotes $p < 0.001$ compared to other compositions).

Conc. (% w/w)			Droplet diameter (µm)			CV (%)		
O	SM	W	D_{10}	D_{50}	D_{90}	D_{10}	D_{50}	D_{90}
10	30	60	0.32 (0.00)*	4.32 (0.03)*	7.74 (0.10)*	0.97	0.66	1.23
10	40	50	1.92 (0.04)*	4.91 (0.01)*	10.6 (0.51)*	2.29	0.29	4.78
10	60	30	0.65 (0.14)	3.27 (0.04)*	5.41 (0.10)*	22.0	1.28	1.89
20	30	50	1.55 (0.02)*	11.18 (0.08)*	25.6 (0.09)*	1.21	0.67	0.37
20	40	40	0.64 (0.02)	10.50 (0.09)*	29.5 (0.30)*	3.89	0.81	1.03
30	40	30	1.41 (0.01)*	23.24 (0.05)*	42.2 (0.53)*	0.60	0.23	1.26

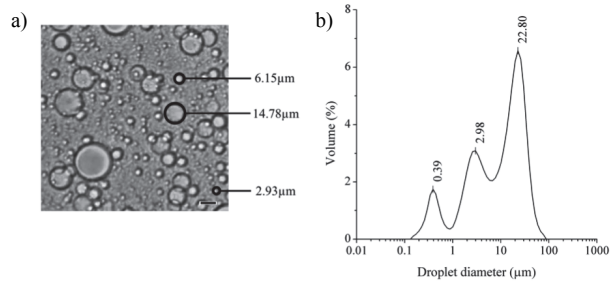

Figure 1. Typical droplet diameters obtained by **a)** light microscopy and **b)** laser diffractometry for a representative composition of 20% w/w RBO, 40% w/w SM and 40% w/w water. Scale bar represents 10 µm.

Scattering pattern of compositions

The scattering patterns observed when the 5 µm microparticles were diluted to 0.1%, 0.05% and 0.03% in distilled water (w/v) are shown in Fig. 2a. Clear peaks were observed at particle concentrations of 0.05% w/v and 0.03% w/v. Similarly, peaks were clearest when Intralipid® was diluted to 0.02% w/v and 0.04% w/v (Fig. 2b).

No differences in scattering pattern were observed at different frequencies for any of the emulsion compositions (Fig. 3), which were diluted by a factor of 2000 to avoid multiple light scattering, a known limiting factor in the application of SALS to rheology[11].

Dilution results in a larger spatial distance between droplets and is therefore expected to alter droplet characteristics. If some sort of aggregation were responsible for the peaks, this would not occur in these dilute conditions. In addition, the diluted compositions had little rheological structure (Fig. 4).

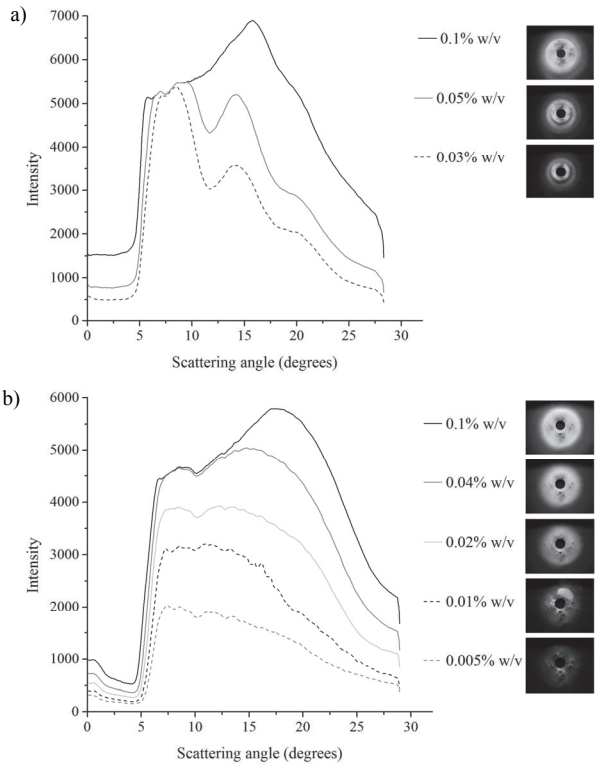

Figure 2. Averaged images after water subtraction and resulting scattering patterns observed when diluting **a)** 5 µm particles and **b)** Intralipid® emulsion at different particle concentrations.

A previous investigation of the rheological properties of undiluted emulsions showed that RBO compositions containing less than 40% w/w SM had

frequency-dependent behaviour, where the G" dominated G' at oscillatory frequencies below 5 Hz (tan $\delta > 1$) and elastic behaviour dominated at higher oscillatory frequencies (tan $\delta < 1$)[9] in a similar pattern to that observed for natural saliva[12,13]. Previously, a reversible peak in G' and G" was observed at a frequency dependent on composition, but this was not observed in the diluted compositions, which may explain the lack of change in microstructure.

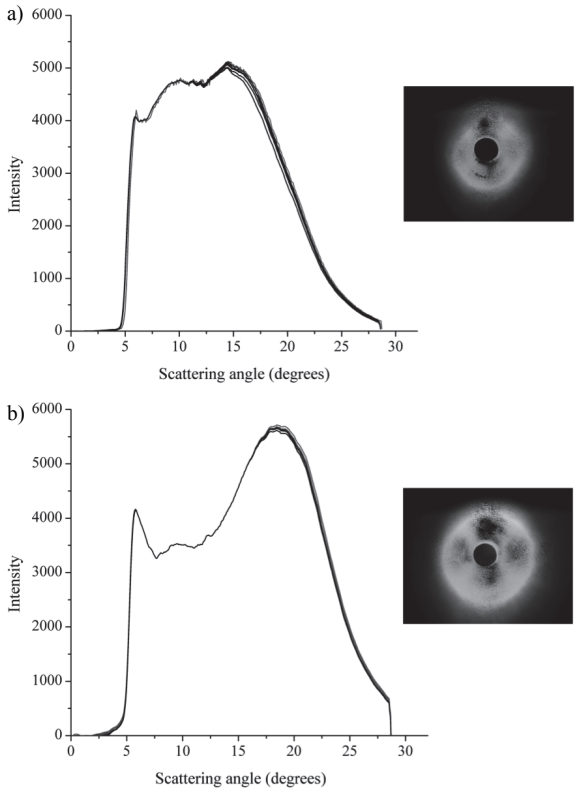

Figure 3. Typical scattering patterns at frequencies of 0.1, 2, 4, 6, 8 and 10 Hz of compositions with a weight ratio of **a)** 20% RBO, 40% SM, 40% water and **b)** 20% RBO, 30% SM, 50% water. Averaged images with water subtracted are shown at a representative frequency of 6 Hz.

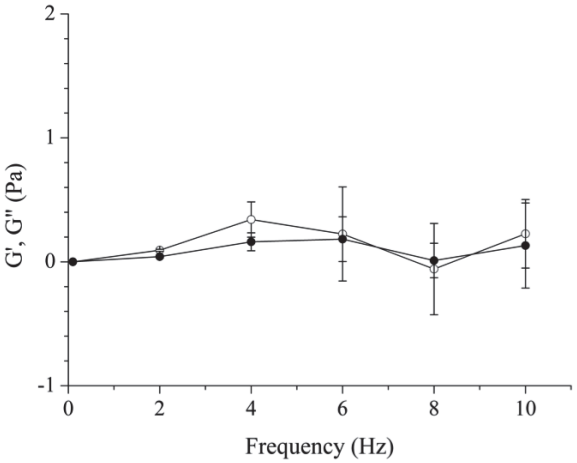

Figure 4. Viscoelastic profile (mean ± SD; n=5) of a composition of 30% RBO, 40% SM and 30% water (w/w), showing typical G' (○) and G" (●) of compositions diluted by a factor of 2000 for SALS.

Different light scattering patterns were observed between compositions (Fig. 5), where at any given frequency, compositions with a higher SM concentration had higher peak intensities. As the wavelength was fixed, the light intensity observed at any scattering angle was dependent on droplet diameter, as well as destructive or constructive interference between transmitted and reflected light[14]. In scattering measurements, peak intensity of smaller particles occurs at larger angles. As particle diameter increases, this peak is observed at smaller angles[15]. Therefore, a higher peak angle is associated with a smaller droplet size. In the present study, droplet size was inversely proportional to SM concentration and indeed, peaks were observed at larger angles in compositions containing 20% w/w RBO with a SM concentration of 40% w/w compared to 30% w/w (Fig. 5). This corresponded with the D_{50} values, which were 11.18 ± 0.08 μm and 10.50 ± 0.09 μm for the compositions containing 40% w/w and 30% w/w SM, respectively (Table 1).

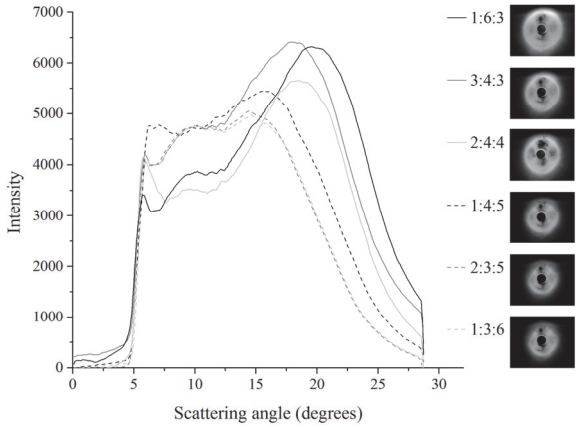

Figure 5. Typical SALS image and corresponding scattering pattern of compositions composed of different weight ratios (w/w) of RBO:SM:water, at a representative frequency of 8 Hz.

CONCLUSION

The droplet size distribution of the tested compositions were biomodal or trimodal, depending on their composition. Droplet size was similar using both light microscopy and laser diffraction. Rheologically structured RBO compositions may offer superior relief in patients with xerostomia, whereby viscous behaviour observed at lower frequencies may improve lubrication of the oral cavity whereas elasticity at higher frequencies may improve retention during chewing and swallowing. SALS could be used to differentiate between formulations, but further work is required to optimise this technique for application in the quantification of changes in droplet microstructure within compositions.

ACKNOWLEDGMENTS

Thank you to the University of Otago School of Pharmacy for a scholarship for SH.

REFERENCES

1. Corcoran RA, Stovell AG, Urquhart D, Chui T, Richardson M (2006), "Evaluation of a combined polymer system for use in relieving the symptoms of xerostomia", *J Clin Dent* **17**(2), 34-38.

2. Vissink A, Waterman HA, 's-Gravenmade EJ, Panders AK, Vermey A (1984), "Rheological properties of saliva substitutes containing mucin, carboxymethylcellulose or polyethylenoxide", *J Oral Pathol Med* **13**(1), 22-28.

3. Yakubov GE, McColl J, Bongaerts JHH, Ramsden JJ (2009), "Viscous boundary lubrication of hydrophobic surfaces by mucin", *Langmuir* **25**(4), 2313-2321.

4. Ranc H, Elkhyat A, Servais C, Mac-Mary S, Launay B, Humbert P (2006), "Friction coefficient and wettability of oral mucosal tissue: Changes induced by a salivary layer", *Colloid Surface A* **276**(1-3), 155-161.

5. Fox PC, van der Ven PF, Sonies BC, Weiffenbach JM, Baum BJ (1985), "Xerostomia: Evaluation of a symptom with increasing significance", *J Am Dent Assoc* **110**(4), 519-525.

6. Nederfors T (2000), "Xerostomia and hyposalivation", *Adv Dent Res* **14**(1), 48.

7. Ferguson MM, Barker MJ (1994), "Saliva substitutes in the management of salivary gland dysfunction", *Adv Drug Deliver Rev* **13**(1-2), 151-159.

8. Mese H, Matsuo R (2007), "Salivary secretion, taste and hyposalivation", *J Oral Rehabil* **34**(10), 711-723.

9. Hanning SM, Yu T, Jones DS, Andrews GP, Kieser JA, Medlicott NJ (2013), "Lecithin-based emulsions for potential use as saliva substitutes in patients with xerostomia - viscoelastic properties", *Int J Pharm* **456**(2), 560-568.

10. USP-NF. 2006. United States Pharmacopeia National Formulary. Laser

diffraction measurement of particle size, ed., Rockville, MD: United States Pharmacopeia Convention. p 2572.

11. Alexander M, Dalgleish D (2006), "Dynamic light scattering techniques and their applications in food science", *Food biophys* **1**(1), 2-13.

12. Stokes J, Davies G (2007), "Viscoelasticity of human whole saliva collected after acid and mechanical stimulation", *Biorheology* **44**(3), 141-160.

13. Hanning S, Motoi L, Medlicott N, Swindells S (2012), "A device for the collection of submandibular saliva", *N Z Dent J* **108**(1), 4-8.

14. Olesik JW, Kinzer JA (2006), "Measurement of monodisperse droplet desolvation in an inductively coupled plasma using droplet size dependent peaks in Mie scattering intensity", *Spectrochim Acta B* **61**(6), 696-704.

15. Deyrail Y, Huneault MA, Bousmina M (2009), "Rheo-optical study of nonlinear effects in an immiscible Newtonian polymer blend under large amplitude oscillatory shear flow", *J Polym Sci Pol Phys* **47**(15), 1467-1480.